Extraction of Sea-State Parameters with an X-Band Radar

☐ **WU Xiongbin, WU Yanqin, CHENG Feng, OUYANG Wenjie, KE Hengyu**

School of Electronic Information, Wuhan University, Wuhan 430072, Hubei, China

Abstract: Ocean wave spectrum and surface currents can be determined from a series of spatial wave images recorded by an X-band marine radar. In the absence of a surface current, the three-dimensional spectral energy found by using the series of images will be confined to a trajectory defined by the still water dispersion relationship. The presence of a surface current will make the three-dimensional spectral energy show a corresponding Doppler shift which may determine the current using the least squares method and obtain the directional wave spectrum. On the basis of conventional wave spectrum and directional function, the paper emulates a series of X-band radar images considering shadowing modulation and simulates numerically the three-dimensional image spectrum both with and without a surface current, calculates the current velocity by virtue of the Doppler shift, and obtains the two-dimensional image spectrum. Finally the paper analyzes measured wave level elevation—a function of time t to obtain one-dimensional image spectrum, and the data comes from an X-band radar in McMaster University.

Key words: X-band radar; Fourier transform; wave spectrum

CLC number: TN 957.51

0 Introduction

The conception of spectrum is mainly relied on to study the random process-ocean waves. Due to spectral analysis, lots of ocean surface parameters can be determined for the purpose of wave prediction, the research of ocean environment and so on. Note that the conventional methods such as buoy can not inspect large ocean area for real time application, ocean remote sensing working as an alternative have caused extensive interest in recent years.

As a remote sensing technique, just like satellites and synthetic aperture radar (SAR), X-band radar can be used as a powerful tool for collecting and analyzing the ocean data[1-4]. When a marine radar detects an ocean target, wave will give returns, named sea clutter, to aggravate the radar detecting abilities awfully. At large angles of incidence, the clutter is mainly due to Bragg resonant backscatter. It is known that Bragg scattering is caused by such wave columns that travel towards or against the radar and have a wavelength being half of the electromagnetic wavelength. X-band marine radars is of about 3 cm electromagnetic wavelength, so it is the gravity capillary wave that makes the clutter. And other waves of longer wavelength can also be seen from the X-band radar images by nonlinear modulations to capillary waves. These modulations mainly are[3,5]: ① Hydrodynamic modulation, which is energy modulation to capillary waves placed by longer waves ; ② Tilt modulation, which is caused by the change of effective incidence angles of radar wave beams due to the slope of longer waves; ③ Shadowing, which produces shadowed areas in the radar images. Peaks of the longer waves obstruct some radar beams, so that sheltered areas

can not give returns and cause the shadowing parts in the images.

Young and other researchers put forward a 3-D Fourier transformation to a series of consecutive radar images considering the gravity wave dispersion relationship[2]. The time variable t was introduced to obtain a 3-D spectrum which removes the directional ambiguity, and the surface current could be extracted from the deviation to the shell defined by the still water dispersion relationship[6-11].

1 Analysis Theory

1.1 Three-Dimensional Discrete Fourier Analysis

The wave level elevation $\eta(\boldsymbol{\xi})$，$\boldsymbol{\xi}$ is a three dimensional vector (x, y, t), x and y are spatial coordinates，t is time. The Fourier transformation of the wave elevation is[2]：

$$\Psi(\boldsymbol{\Omega}) = \sum_{j=0}^{N-1} \eta(\boldsymbol{\xi}_j)\exp(-\mathrm{i}\boldsymbol{\Omega}\cdot\boldsymbol{\xi}_j) \qquad (1)$$

where $\boldsymbol{\Omega}$ is the wave number frequency vector，vector product $\boldsymbol{\xi}_j\cdot\boldsymbol{\Omega}=k_x x+k_y y-\omega t$. $\eta(\boldsymbol{\xi})$ is a real function. The complex conjugated form of Eq.(1)：

$$\Psi^*(\boldsymbol{\Omega}) = \sum_{j=0}^{N-1} \eta(\boldsymbol{\xi}_j)\exp(\mathrm{i}\boldsymbol{\Omega}\cdot\boldsymbol{\xi}_j) \qquad (2)$$

From Eq.(1) and Eq.(2)：

$$\Psi(\boldsymbol{\Omega}) = \Psi^*(-\boldsymbol{\Omega}) \qquad (3)$$

According to the Fourier transformation，the wave number spectrum can be defined as：

$$\Gamma(\boldsymbol{\Omega}) = \frac{1}{M_x M_y T}\left|\Psi(\boldsymbol{\Omega})\right|^2 \qquad (4)$$

where M_x and M_y are the maximum value of coordinates x and y, T is the length of time series.

From Eq.(3) and Eq.(4)：

$$\Gamma(\boldsymbol{\Omega}) = \Gamma(-\boldsymbol{\Omega}) \qquad (5)$$

hence spectrum $\Gamma(\boldsymbol{\Omega})$ is symmetric about the zero point in (k_x, k_y, ω) space. If $\boldsymbol{\Omega}$ is vector (k_x, k_y), Eq.(5) becomes $\Gamma(k_x, k_y)=\Gamma(-k_x, -k_y)$, which is difficult to determine whether the waves propagate in (k_x, k_y) direction or $(-k_x, -k_y)$ direction, named 180 degrees directional ambiguity. For three-dimensional Fourier analysis, Eq.(5) is $\Gamma(k_x, k_y, \omega)=\Gamma(-k_x, -k_y, -\omega)$, so given the value of ω, a unique spectrum will be shown without the directional ambiguity.

On one half plane $\omega>0$, the integration of Eq.(4) can obtain the two-dimensional wave number spectrum $\Gamma(k_x, k_y)$：

$$\Gamma(k_x, k_y) = \int_{0}^{\infty}\Gamma(k_x, k_y, \omega)\mathrm{d}\omega \qquad (6)$$

As $\boldsymbol{k}$ and ω follow the dispersion relationship, $\boldsymbol{k}$ is a function of ω. Hence $\Gamma(k_x, k_y)$ can be changed to another common two-dimensional form $\Gamma(f, \theta)$ and integrated to $\Gamma(f)$，where θ is the angle in the polar coordinate of $\boldsymbol{k}$.

$\Gamma(f)$ is

$$\Gamma(f) = \int_{0}^{2\pi}\Gamma(f, \theta)\mathrm{d}\theta \qquad (7)$$

1.2 Dispersion Relationship

Assume that gravity waves follow the first order approximation of the dispersion relationship:

$$\omega_0{}^2 = g\left|\boldsymbol{k}\right|\tanh(\left|\boldsymbol{k}\right|d) \qquad (8)$$

where $\boldsymbol{k}$ is the wave number vector, d is the depth of ocean, g is the gravitational acceleration. The presence of a current $\boldsymbol{U}$ will cause a Doppler shift, which alters the relationship between $\boldsymbol{k}$ and ω:

$$\omega = \omega_0 + \boldsymbol{k}\cdot\boldsymbol{U} \qquad (9)$$

Figure 1 shows the dispersion relationships defined by Eq.(8) and Eq.(9) respectively.
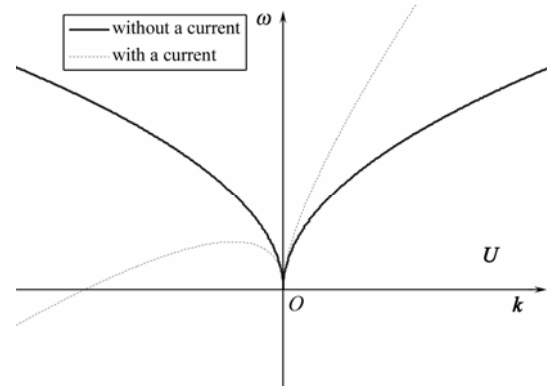

Fig.1 A scheme of the dispersion relationships defined by Eq.(8) and Eq.(9) respectively

Note: The solid line is the plot of still water dispersion relationship, the dashed line is the plot of dispersion relationship in the presence of a current. $\boldsymbol{k}$ and $\boldsymbol{U}$ propagating in the same direction is assumed

For a given value of frequency, in the presence of a current, the values of the wave number on positive half plane $(k>0)$ show a general decline when compared with those limited by the still water dispersion relationship.

In the three-dimensional Fourier analysis, the energy density spectrum distributes on the shell defined by the dispersion relationship. The three-dimensional spectrum has vanishing values when the corresponding k and ω does not fit the dispersion relationship Eq.(8) or Eq.(9). This is a filtering mechanism, behaving like a δ function and Eq.(6) becomes:

$$\Gamma(\boldsymbol{k}) = \int_{\omega'>0} \Gamma(\boldsymbol{k},\omega')\delta(\omega'-\omega(\boldsymbol{k},d,\boldsymbol{U})){\rm d}\omega' \qquad (10)$$

thus a current can be extracted from the deviation to the still water dispersion relationship. A least square method can be used to find appropriate values (U_x, U_y) filled in Eq.(9) to fit the curve closest to the distribution of spectrum.

2 The Model of X-Band Radar Image Sequence

2.1 Longuet-Higgins Model

During a relative short time, the ocean wave can be viewed as a quasi-stationary random process. Longuet-Higgins model[9] gives a description of a fixed point within ocean areas by summing up numerous random waves:

$$\eta(t) = \sum_{n=1}^{\infty} a_n \cos(\omega_n t + \varepsilon_n) \qquad (11)$$

where a_n is the wave's amplitude, ω_n is the angular frequency, ε_n is the random initial phase following a uniform distribution between 0 and 2π.

Wave spectrum density function $S(\omega)$ and a_n as follows:

$$S(\omega) = \frac{1}{\Delta\omega} \sum_{\omega}^{\omega+\Delta\omega} \frac{1}{2} a_n^2 \qquad (12)$$

Eq.(11) does not inspect large areas of ocean surface in different wave directions. In fact, the three-dimensional wave energy distributes in a large angular scope. Hence ocean waves can be summed up by many simple cosine waves with amplitude a_{ij}, angular frequency ω_i and initial phase ε_{ij}. Especially assume that these waves propagate along angle θ_j with respect to x axis on the x, y horizontal spatial plane:

$$\eta(x,y,t) = \sum_{i=1}^{n}\sum_{j=1}^{m} a_{ij} \cos[\omega_i t - k_i(x\cos\theta_j + y\sin\theta_j) + \varepsilon_{ij}] \quad (13)$$

where, k_i and ω_i follow the dispersion relationship Eq.(8) or Eq.(9).

The directional spectrum density function $S(\omega,\theta)$ can be related to a_n by:

$$a_{ij} = \sqrt{2S(\omega_i,\theta_j)\Delta\omega\Delta\theta} \qquad (14)$$

In general, the directional spectrum is written in the form:

$$S(\omega,\theta) = S(\omega)G(\omega,\theta) \qquad (15)$$

where $S(\omega)$ is the wave spectrum, $G(\omega,\theta)$ is the directional distributed function.

It is important to choose appropriate directional wave spectrum to emulate real ocean waves, including the wave spectrum and directional function. This paper selects Pierson-Moscowitz (PM) spectra to complete the wave model. PM spectra is:

$$S(\omega) = \frac{ag^2}{\omega^5} \exp[-\beta(\frac{g}{U\omega})^4] \qquad (16)$$

where the constant $a = 8.1\times10^{-3}$, $\beta = 0.74$, g is the gravitational acceleration, U is the wind velocity above ocean surface 19.5 m. The PM spectrum is a narrow band spectrum and its main energy centers within a certain frequency interval. The peak frequency of the spectra can be derived from $\frac{\partial S(\omega)}{\partial\omega} = 0$[7]:

$$\omega_m = \frac{8.565}{U} \qquad (17)$$

hence ω_m decreases when U increases.

And this paper selects the directional function in SWOP(Stereo Wave Observation Project) spectra to build ocean wave model that needed. This directional function is:

$$G(\omega,\theta) = \frac{1}{\pi}(1 + p\cos 2\theta + q\cos 4\theta) \qquad (18)$$

where $p = \left(0.50 + 0.82\exp[-\frac{1}{2}(\frac{\omega}{\omega_m})]^4\right) S(f,\theta)/S_{\max}$, $q = 0.32\exp\left[-\frac{1}{2}(\frac{\omega}{\omega_m})^4\right]$, $|\theta| \leqslant \pi/2$.

Figure 2 shows a three-dimensional plot of the directional wave spectrum at 10 m/s wind speed in the frequency direction space.
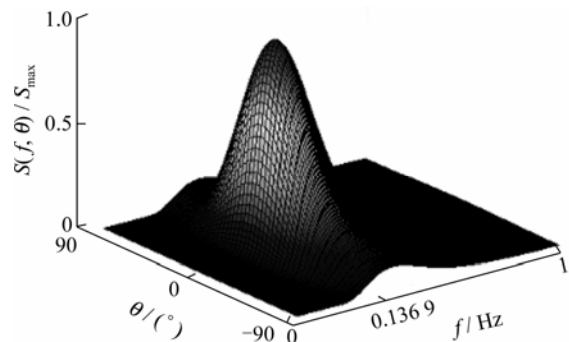

Fig.2   The directional wave spectrum

2.2 Simulation of Radar Images

With the PM spectra and directional function of SWOP spectra, this paper uses discrete-valued frequencies and angles in Eq.(13) to determine the wave models. Assume that: ① The water depth is infinite; ② Radar is mounted on the seashore at a height of 150 m; ③ The measuring distance is from 1 000 to 1 635 m; ④ The radar images is only modulated by shadowing.

Figure 3(a) shows a still water radar image of the ocean waves which are summed up by 240 cosine waves. The parameters of these cosine waves include 15 discrete frequencies distributed in the interval(0.016 7,0.483 3)
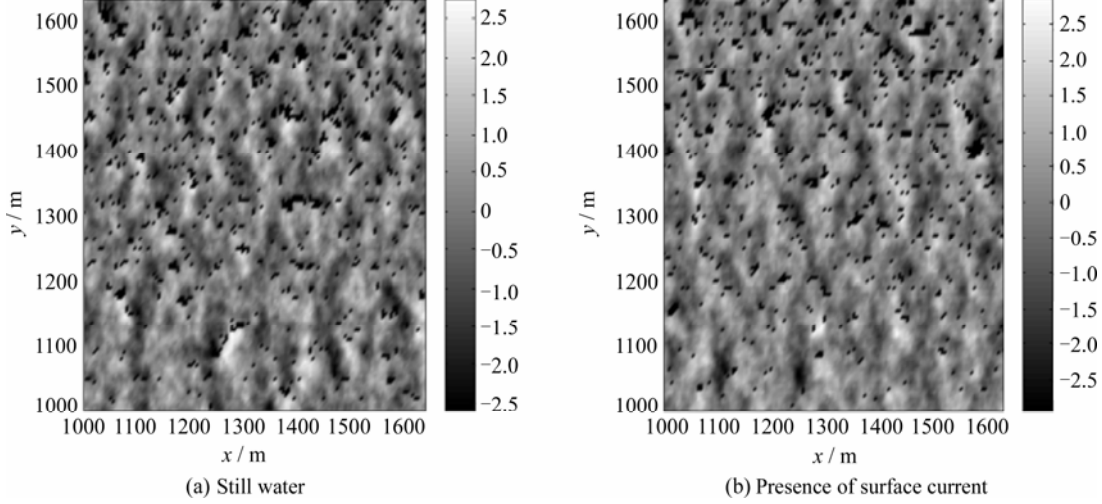
Hz and 16 discrete directional angles lie in the interval $(-90°, 90°)$.

Figure 3(b) shows a plot of a radar image in the presence of a surface current $U_x = 0.25$ m/s, $U_y = 0.5$ m/s.

(a) Still water

(b) Presence of surface current

Fig.3   Simulated X-band radar image

3　Numerical Test of Fourier Analysis Method

3.1　Fourier Analysis of Radar Images without a Current

The wave spectral energy is concentrated in narrow bands of frequency, thus the maximum sampling period can be determined in terms of Shannon theorem. If τ is the sampling period, ω_n is the maximum angular frequency of $S(\omega)$, then τ and ω_n must follow $\omega_n \leqslant \pi / \tau$. Thus when PM spectra at a wind velocity of 10 m/s can obtain $\omega_n \approx 3$ rad/s, the sampling period τ will be 1 s accordingly.

This paper selects 30 consecutive radar images of wave models established in Section 2, representing 30 s of data in the absence of a current. This time length yields angular frequency resolution dω=0.209 3 rad/s. On (x, y) horizontal spatial plane, each image consists of 128×128 pixels with spatial resolution dx=dy=5 m, yielding wave number resolution dk=9.813×10^{-3} rad/m.

From Eq.(1) and Eq.(4), 30 radar images are Fourier transformed to evaluate the three-dimensional image spectrum. The circles in Fig.4 is the curves of still water dispersion relationship.

Since the wind velocity is 10 m/s, the peak frequency of PM spectra is 0.856 5 rad/s (that is 0.136 4 Hz) derived from Eq.(17). Considering the narrow-band

spectral character, the spectrum concentrates within the interval ranging from 0.11 to 0.17 Hz. As direction angles are assumed to distribute in $(-90°, 90°)$, the spectral value all lie on the right half plane $(k_x > 0)$ and fit well with the still water dispersion relationship circle.

3.2　Determination of Directional Wave Spectrum

The two-dimensional wave number spectrum $\Gamma(k_x, k_y)$ can be derived from Eq.(10), and changed to another alternative form $\Gamma(f, \theta)$. The three-dimensional image spectrum deduced in the absence of a current in Fig.4 will be analyzed here. Figure 5 shows the contour plot of the two-dimensional image spectrum in frequency-direction space. The energy distribution almost reflects the narrow-band characteristics of the directional wave spectrum (Fig.2) used for wave simulation, which is concentrated near 0° and 0.15 Hz.

One-dimensional spectrum $\Gamma(f)$ can be estimated by Eq.(7).The normalized result in frequency space and PM spectra S used for simulation both are shown in Fig.6.

A significant difference of the normalized energy can be seen in Fig.6 due to the shadowing modulation. These nonlinear modulations make the radar data perturbed from ocean wave level elevations and cause errors in the Fourier analysis. Then a modulation transfer function(MTF) is needed to transform the two-dimensional image spectrum into the two-dimensional wave spectrum[3,4]. From the two-dimensional wave spectrum all important sea state parameters can be derived in real time.
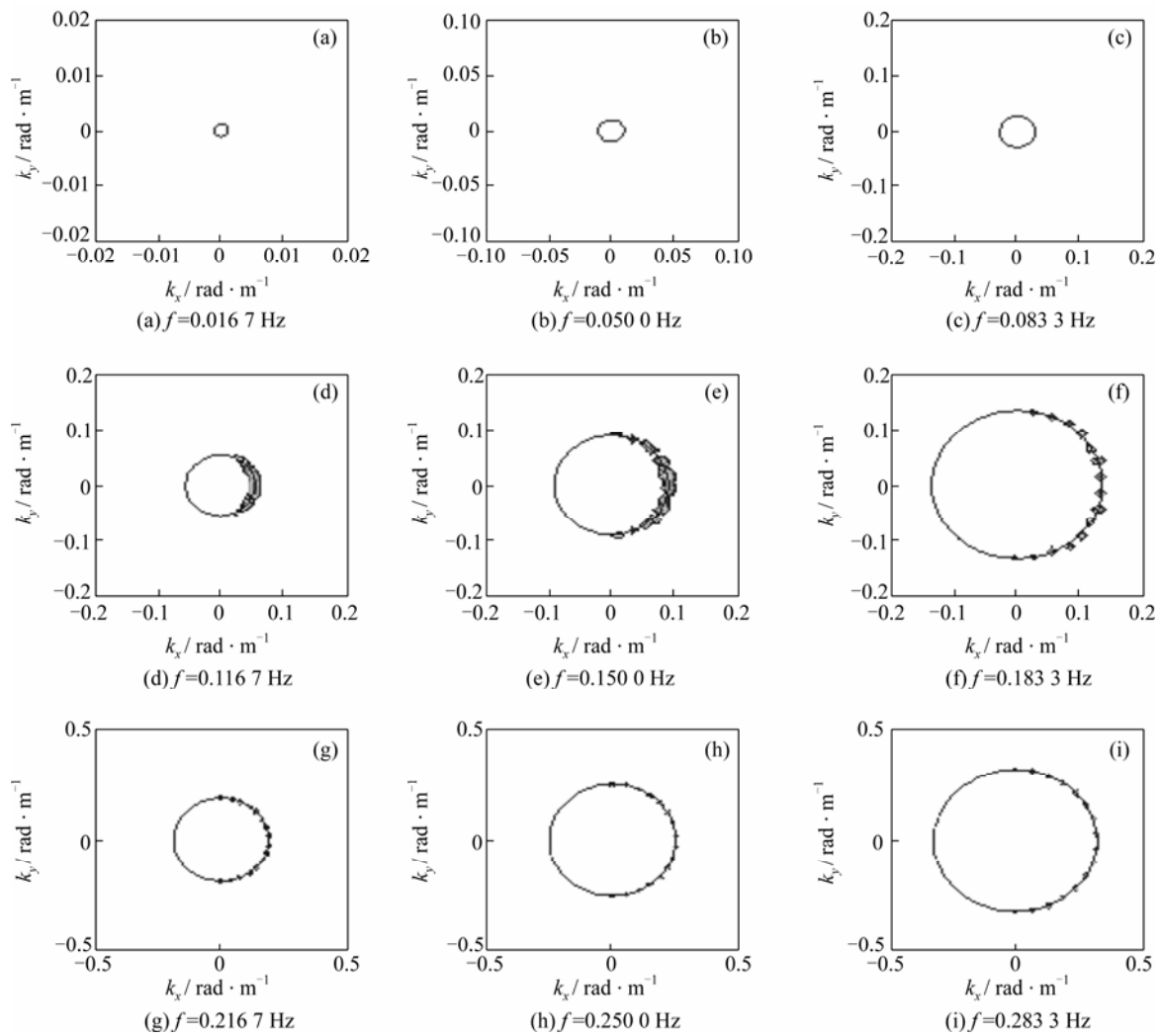
Fig.4   The contour plot of three-dimensional image spectrum for a given frequency with the still water dispersion relationship (round circle) and the absence of a current
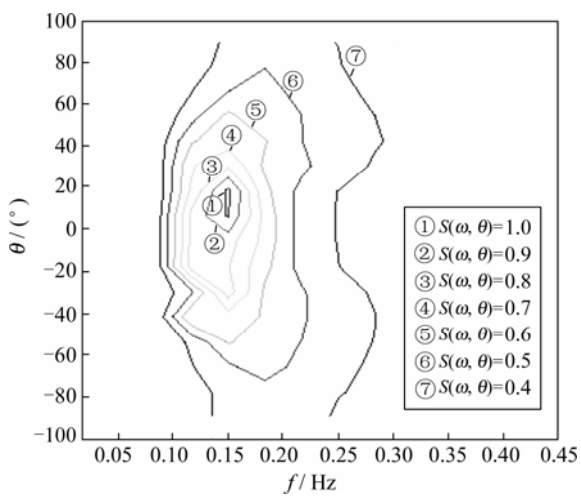

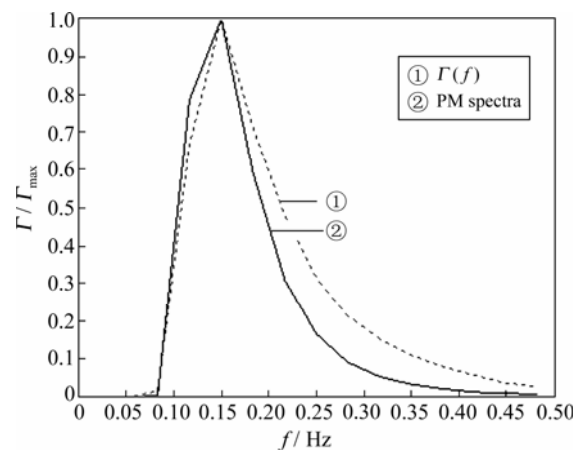**Fig.5   A contour plot of the two-dimensional spectrum**

Fig.6   The comparison of the result spectrum $\Gamma(f)$ (dashed line) and PM spectra (solid line) used for simulation

3.3   The Extraction of Surface Currents

A current will cause a Doppler shift to the distribution of spectral energy. Figure 7 shows the contour plot of 30 radar images simulated in Fig.3 superimposed by the still water dispersion relationship.

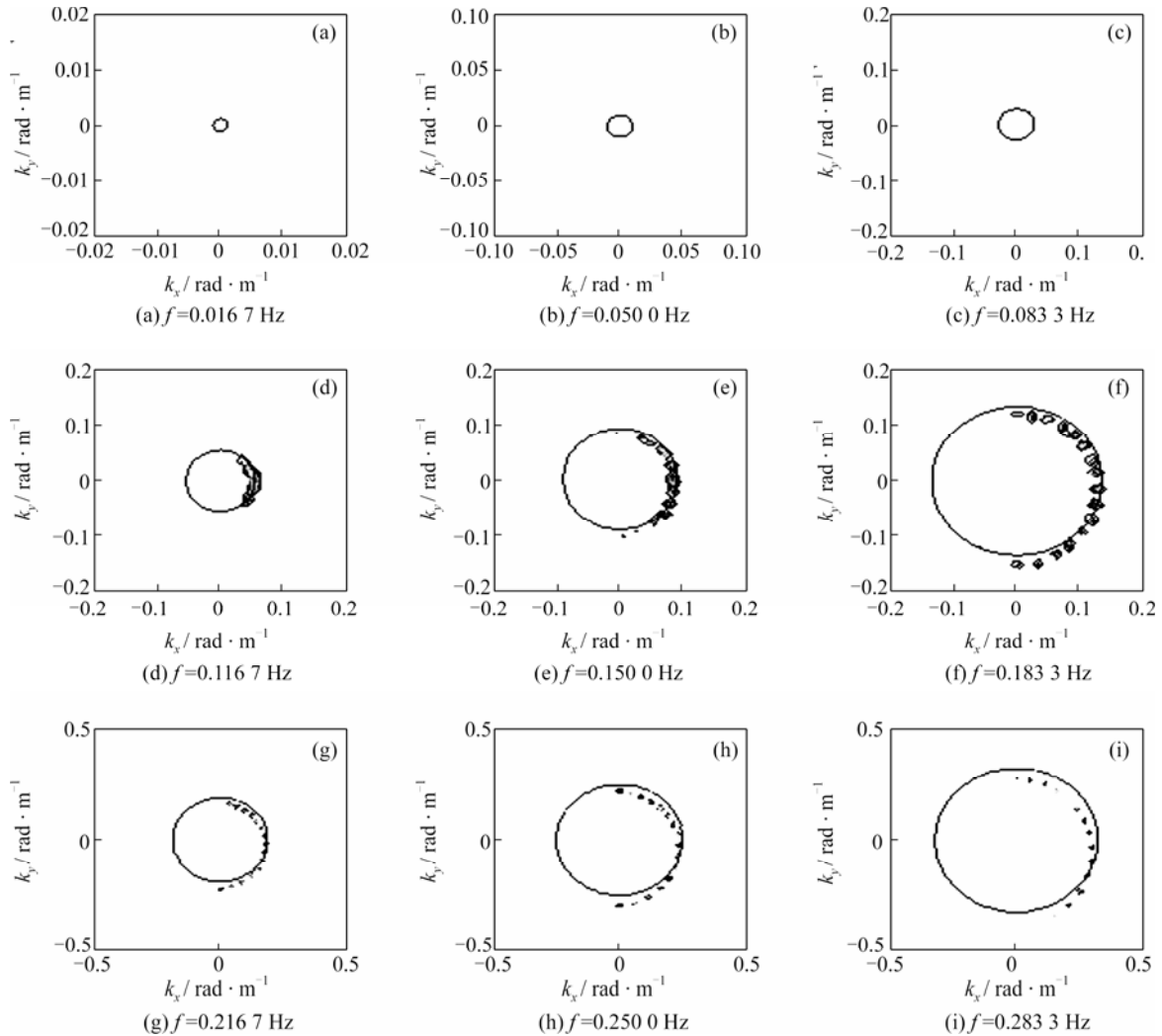The deviation from the still water dispersion rela

Fig.7   The contour plot of three-dimensional image spectrum for a given frequency with the still water dispersion relationship (round circle). (Note a current do exist)

tionship is due to the presence of a current, hence a least square method is used to analyze this shift to evaluate the current. In this paper, the analysis yields $U_x = 0.246\ 7$ m/s, $U_y = 0.491\ 6$ m/s, with relative bias $d_x = -1.32\%$, $d_y = -1.68\%$ compared with the true data which is assumed in Section 2.The distributions of spectral energy for any given frequencies less than 0.150 0 Hz are not taken into account, so as to avoid errors due to data ambiguities.

The dispersion relationship is modified into the form $\omega = \omega_0 + U_x k_x + U_y k_y$ with the estimated value of the current. After least square fitting, the spectra contours will locate in coincidence with the circle of still water dispersion relationship.

4   Fourier Analysis of the Measured Data

The data was measured when McMaster IPIX Radar was working in the mode of two minute stare. This fully coherent X-band radar is developed in McMaster University, with features of dual transmit/receive polarization and high resolution. Since the radar is operated in the mode of stare, not surveillance which records two-dimensional spacial radar images, this paper could only obtain one-dimensional spectrum utilizing the data in the staring direction. The Fourier analysis form is similar to Eq.(1):

$$\Psi(\omega) = \sum_{j=0}^{N-1} \eta(t) \exp(-\mathrm{i}\omega t) \tag{19}$$

One-dimensional image spectrum $E(\omega)$ can be obtained by normalize the square of the modulus of $\Psi(\omega)$. This method is equivalent to the periodogram method due to the mathematics expression of $E(\omega)$.

The radar data was measured by staring in a direction for 131.072 s (radar specifications are in Table 1) when overlooking the Atlantic Ocean from a clifftop in Dartmouth, Nova Scotia.

Table 1   Properties of the radar

Frequency/GHz	9.39
Pulse length/ns	200
Pulse repetition frequency/Hz	1 000
Polarization	HV or VH

According to the experiment record, the returns from the 7 to 10th range cells are affected by a weak target, which is a spherical block of Styrofoam, wrapped with wire mesh. Since the target strengthens sea echo signals, this paper selects radar data from these four range cells to be Fourier analyzed and obtain one-dimensional spectrum respectively. Figure 8 gives a plot of the average of four spectrum obtained above and the values are normalized. In order to smooth the spectral curve, the paper utilizes Welch-Bartlett periodogram method. The 131 072 samples in each range cell are segmented into five 50 % overlapping blocks, reducing the spectrum variance at the cost of spectral resolution.
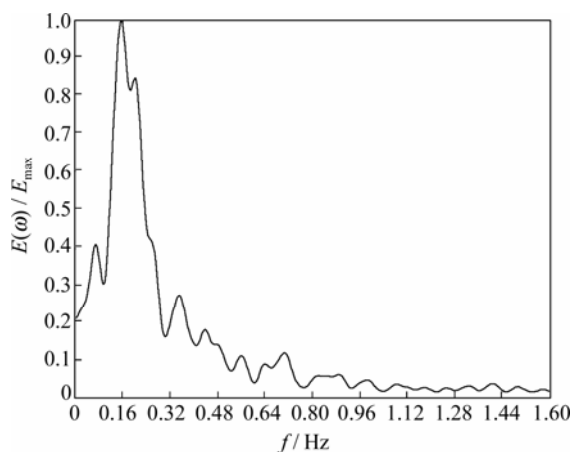

Fig.8   The normalized average of spectrum obtained in four range cells

5   Conclusion

X-band radar images are mainly generated by capillary waves fulfilling Bragg scattering criterion, and longer waves could be also visible for they modulate the echo signals.On the basis of spatial and temporal homogeneity within the observed area, a discrete Fourier transformation is used to analyze the digital series of radar images and obtain three-dimensional image spectrum. The comparison of theoretical and empirical location of the spectral energy can be used to calculate the ocean current, which could modify the dispersion relationship. Integral of the three-dimensional spectrum will obtain the two-dimensional directional spectrum and then one-dimensional spectrum, from which lots of ocean parameters such as wave height and period may be derived in real time. X-band radar can be applied in various fields like navigation and fishery, thus it is a prosperous research program.

References

[1]   Hoogeboom H, Rosenthal P W. Directional Wave Spectra in Radar Images[C] //*The International Geoscience and Remote Sensing Symposium*, *IEEE Geosci and Remote Sensing So*. Munich: IEEE Press, 1982.

[2]   Young I R, Rosenthal W, Ziemer F. Three-Dimensional Analysis of Marine Radar Images for the Determination of Ocean Wave Directionality and Surface Currents [J]. *J Geophys Res*, 1985, **90 (**C1**)**: 1049-1059.

[3]   Borge J C, Rodriguez G R. Inversion of Marine Radar Images for Surface Wave Analysis[J]. *American Meteorological Society*, 2004, **21**(8): 1291-1300.

[4]   Borge J C. *Estimation of the Significant Wave Height with X-Band Nautical Radars*[R]. St. John's: Ocean, Offshore and Arctic Engineering (OOAE) Division, 1999.

[5]   Stewart R H. *Physical Oceanography*[M]. Beijing: China Ocean Press, 1992(Ch).

[6]   Valenzuela G R. Theories for the Interaction of Electromagnetic and Ocean Waves—A Review[J]. *Boundary Layer Meteorolog*, 1978, **13**: 61-85.

[7]   Lee P H Y. X Band Microwave Backscattering from Ocean Waves[J]. *Journal of Geophysical Research*, 1995, **100** (C2): 2591-2611.

[8]   Yang Huaiping, Sun Jiaguang.Wave Simulation Based on Ocean Wave Spectrums[J]. *Journal of System Simulation*, 2002, **14** (9): 1175-1178(Ch).

[9]   Li Hui, Guo Chen, Li Xiaofang. 3-D Visual Simulation of Irregular Ocean Waves Based on Matlab[J]. *Journal of System Simulation*, 2003, **15** (7): 1057-1059(Ch).

[10]   Wen Shengchang, Yu Zhouwen.*The Theories and Calculations of Ocean Waves*[M]. Beijing: Science Press, 1984 (Ch).

[11]   Manolakis G, Ingle K, Kogon M. *Statistical and Addaptive Signal Processing*[M]. Beijing: Publishing House of Electronics Industry, 2003 (Ch).

□